Synthesis and Characterization of Poly(*N*-Methyl Aniline) Doped with Sulphonic Acids: Their Application as Humidity Sensors

Milind V. Kulkarni, Annamraju Kasi Viswanath, P. K. Khanna

Photonics and Advanced Materials Laboratory, Centre for Materials for Electronics Technology, (C-MET), Panchwati, Off Pashan Road, Pune 411 008, India

Received 10 September 2004; accepted 31 January 2005
DOI 10.1002/app.22585
Published online in Wiley InterScience (www.interscience.wiley.com).

ABSTRACT: Single step chemical polymerization of *N*-methyl aniline was carried out by using ammonium persulphate as an oxidizing agent. The conducting emeraldine salt phase of the polymers using camphor sulfonic acid and *p*-toluene sulfonic acid as dopants was made by a direct process. The polymers were characterized by UV-vis and FTIR spectroscopy, scanning electron microscopy, TGA, and conductivity measurements. The synthesized polymers were found to have very good physicochemical properties and good electrical conductivity. Conductivity measurements have shown "thermal activated behavior." The change in resistance with respect to % relative humidity (RH) was observed, when pressed pellets of the polymer were exposed to the broad range of humidity (ranging between 20 and 100% RH). © 2005 Wiley Periodicals, Inc. J Appl Polym Sci 99: 812–820, 2006

Key words: conducting polymers; electron microscopy; FT-IR; sensors; UV-vis spectroscopy

INTRODUCTION

Inherently conducting polymers (ICPs) or electroactive polymers have attracted a great deal of attention during the past decade because of their unusual electric/electronic properties and for a great potential for commercial applications.[1,2] Among the conducting polymers, polyaniline (Pani) has been the most widely studied material as a unique member of the conducting polymer family for the following reasons:

i. It is the only conducting polymer whose electronic structure and electrical properties can be reversibly controlled by both oxidation and protonation.
ii. It has interesting electrochemical behavior and very high environmental stability[3] and conductivity, together with ease of preparation.[4–6]

However, the industrial development of Pani is considerably hampered by its insolubility in common organic solvents, infusibility, and low mechanical strength or inherent brittleness. Incorporation of polar functional groups or long and flexible alkyl chains in the polymer backbone is a common technique to prepare Pani type polymers that are soluble in water and/or organic solvents. For example, substituted polyanilines, like polytoluidines, polyanisidines, or poly(*N*-methyl), or poly(*N*-ethyl anilines) are more soluble in common organic solvents than the unsubstituted Pani but render low conductivity. Figure 1 shows the structures of unsubstituted polyaniline (a), and polaron (b) and bipolaron (c) forms of substituted polyaniline. In a polyaniline system, polarons are radical cations that govern the transport properties. Thus, polaron is an ordinary radical ion with a unit charge and spin = 1/2. A combination of two polarons in a single chain of polymer is called a bipolaron. Thus, bipolaron consists of two coupled polarons with charge = 2e and spin = 0. The bipolarons are not created directly but must form by the coupling of pre-existing polarons or possibly by the addition of charge to pre-existing polarons. The polarons and bipolarons are mobile, and under the influence of an electric field can move along the polymer chain, from one chain to another and from one granule to another, exactly in the manner electrons and holes do in inorganics. The conductivity in these polymers can be varied by doping them with different protonic acids or by using "suitable functionalized protonic acids," which make the polymers conducting as well as soluble in organic solvents, like toluene, xylene, chloroform, *m*-cresol, and so forth.[7,8]

An accurate and reliable estimate of water vapor in different environments is an important prerequisite

Correspondence to: A. K. Viswanath (v_kasi@hotmail.com).

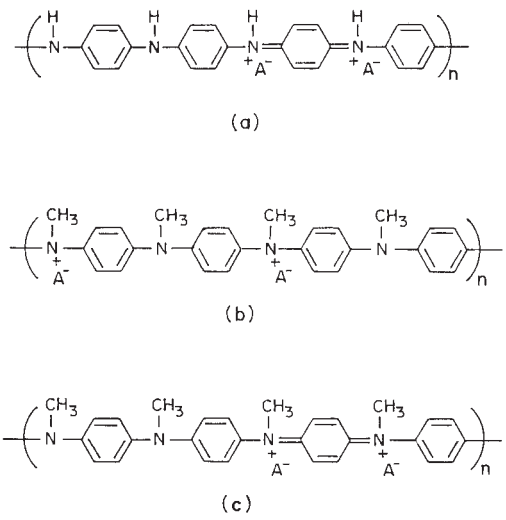

Figure 1 Structures of unsubstituted polyaniline (a) and polaronic (b) and bipolaronic (c) forms of substituted polyaniline.

for a variety of processes, such as agriculture, weather control, drying technology, food processing, textile technology, and so on. Measurement and control of the humidity of the environment are also important for domestic comfort (like air conditioning) and also for the working of several instruments useful for industrial controlled systems. Therefore, humidity sensors have found wide applications in industrial production, process control, environmental monitoring, storage, electrical applications, and so forth,[9] and the research devoted to the development of new materials for sensor devices is gaining more and more attention. Different types of materials, such as electrolytes, porous ceramics, and organic polymers,[10] are currently being used for making humidity sensors. Conducting polymers or π- conjugated polymers possess special electrical and electro-optical properties and have been widely employed in the construction of various types of sensors. Recently, they were also investigated as humidity sensitive materials, and some encouraging results have been obtained.[11,12] We have taken up a systematic investigation of conducting polymers[13–18] and polymers doped with suitable molecules for the development of humidity sensors.[19,20]

Therefore, the aim of the present work is to synthesize poly(*N*-methyl aniline), PNMA, by using CSA and *p*-TSA as dopants and to obtain structural information by studying the physicochemical properties of this polymer using various analytical techniques, such as UV-vis and FT-IR spectroscopy, SEM, TGA, and conductivity measurements. The synthesized polymers were then successfully utilized as humidity sensors for a broad range of humidity ranging between 20 to 100% RH.

EXPERIMENTAL

All chemicals used were of analytical reagent (AR) grade. The solutions were prepared in doubly distilled water. The polymerization of the monomer, *N*-methyl aniline (0.59 mL) was initiated by the drop-wise addition of the oxidizing agent $(NH_4)_2S_2O_8$ (1.26 g) under constant stirring at low temperature between 0 to 5°C in an acidified solution (10 mL) containing 3.08 g of CSA or 1.90 g of *p*-TSA. The monomer to oxidizing agent ratio was kept as 1 : 1. After complete addition of the oxidizing agent, the reaction mixture was kept under constant stirring for 24 h. The greenish-black precipitate of the polymer was then isolated by filtration and conditioned by washing and drying in an oven. UV-vis spectra of the polymer solutions in *m*-cresol were recorded by using a Hitachi-U3210 spectrophotometer in the range of 300–900 nm.

FTIR spectra of the polymers were taken on a Perkin–Elmer-Spectrum 2000 spectrophotometer between 400 and 4000 cm^{-1}. The samples were prepared in the pellet form using spectroscopic grade KBr powder. Morphological studies were performed with the help of a Philips XL-30 Scanning Electron Microscope. The thermogram of the polymer samples was recorded using a Mettler-Toledo 851 thermogravimetric analyzer in the presence of N_2 atmosphere from RT to 900°C with a heating rate of 10°C/min.

The room temperature conductivity was measured by the two probe technique. Dry powdered samples were made into pellets using a steel die having 1.5 cm diameter in a hydraulic press under a pressure of 7 tons. Temperature dependent electrical conductivity of the polymer samples was measured using a laboratory made set up.

Figure 2 shows the schematic diagram of the dynamic humidity chamber used for varying and measuring the humidity by the two temperature method.

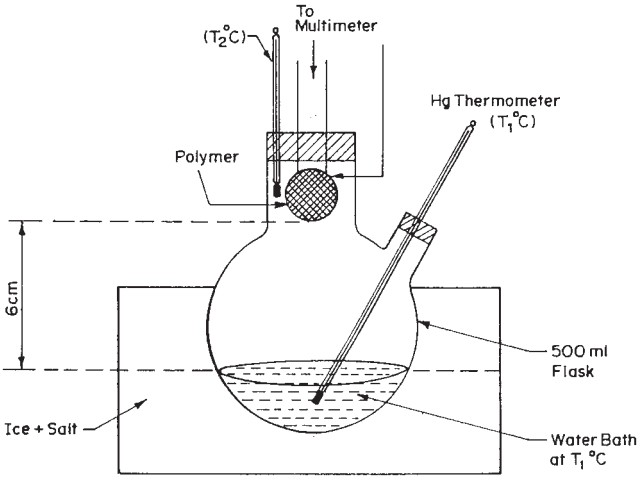

Figure 2 Schematic of the experimental set up for the measurement of % RH (using the two temperature method).

The humidity system used consists of a closed flask (total volume 500 mL) with two necks for inserting thermometers and the sensor. The flask is partially filled with water and kept in a thermocole container. An external container is filled to the equal level of water (which is present in the flask) with ice. The temperature of the system is adjusted by mixing ice and water as required. Thus, the water inside the flask can be kept at the required temperature (T_1). The sensor (i.e., pellets of poly(*N*-methyl aniline)) was mounted inside the flask at a height of 6 cm from the surface of the water, and the temperature of the sample (T_2) was measured with a thermometer placed at an equal height of the sample to be studied.

The humidity inside the chamber is calculated by taking the ratio of the saturated water vapor pressure at water temperature (T_1) and the sample temperature (T_2). The values of the saturated vapor pressure are obtained from the *CRC Handbook of Chemistry and Physics*. It is to be noted that the temperature of the sample changes by 3–6°C during the experiment. The % RH inside the flask is given by

$$\%\mathrm{RH} = \frac{\mathrm{E_w}(T_1)}{\mathrm{E_w}(T_2)} \times 100 \qquad (1)$$

where E_w (T_1) is the saturated water vapor pressure at the temperature of water and E_w (T_2) the saturated water vapor pressure at the temperature of the sensor element. Different % RH values are obtained by adjusting the temperature of the water inside the flask, with ice and water mixture from room temperature to 0°C. The system equilibrium time is small, and stable readings were obtained within 10 min.[20]

RESULTS AND DISCUSSION

UV-vis spectroscopy is a very sensitive tool for the studies of protonation as well as for the elucidation of the interactions between the solvent, the dopant, and the polymer chains. Figure 3 shows the optical absorption spectra of the poly (*N*-methyl aniline) doped with CSA and *p*-TSA by using *m*-cresol as a solvent. In *m*-cresol, poly (*N*-methyl aniline) exhibits three peaks, at 320 nm, 420 nm, and 820 nm. The peak at 320 nm corresponds to the π- π^* transition of the benzenoid rings, while the peak at 420 nm can be attributed to the localized polarons that are the characteristics of the protonated polyaniline. The peak at 820 nm is assigned to the conducting emeraldine salt phase of the polymer.[13] The spectral features in Figure 3 reveal the enhanced solubility of poly (*N*-methyl aniline) in *m*-cresol. The extended tail at higher wavelength depicts that *m*-cresol not only serves as a solvent but also acts as an efficient "secondary dopant."[21,22] MacDiarmid et al.[22] introduced the term efficient "secondary doping"

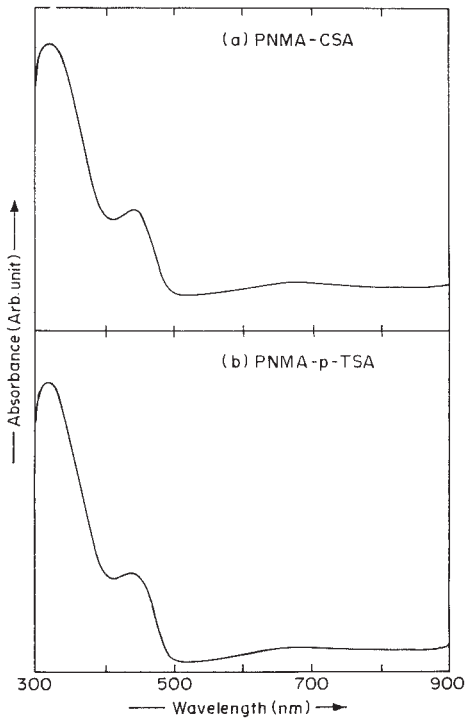

Figure 3 UV-vis spectra of poly(*N*-methyl aniline) doped with CSA (a) and *p*-TSA (b) using *m*-cresol as a solvent.

to describe the interaction of *m*-cresol and other phenols with protonated polyaniline. *m*-Cresol interacts more strongly with the polymer chain and/or with the dopant ion, consistent with a progressive change in molecular conformation from "compact coil" to "extended coil." Figure 4 shows the schematic of the possible interaction of the polymer with *m*-cresol.

In a series of papers, Ikkala et al.[23,24] have used a concept of "supramolecular chemistry" in the explanation of sulfonic acid protonated polyaniline in phenol type solvents. Thus, the formation of the extended chain conformation in protonated polyaniline, which, in turn, favors polaron delocalization, requires strong interaction via hydrogen bonding between the solvent, counter ion, and the polymer chain, together with a geometrical match between the solvent and polymer repeat units, to enhance the van der Walls interaction. This is an attractive concept because it implies that polaron delocalization in polyaniline can be obtained for counter ion-solvent couples, which differ significantly in chemical nature from sulfonic acid anion and phenols, provided that the molecules involved are capable of interacting via hydrogen bonding and the geometrical match conditions are fulfilled.

Figure 5 represents the FTIR spectra of the poly (*N*-methyl aniline) doped with CSA and *p*-TSA, and the peak positions related to the corresponding chemical bonds are listed in Table I. From the Figure as well as from Table I, it is observed that the structure of the

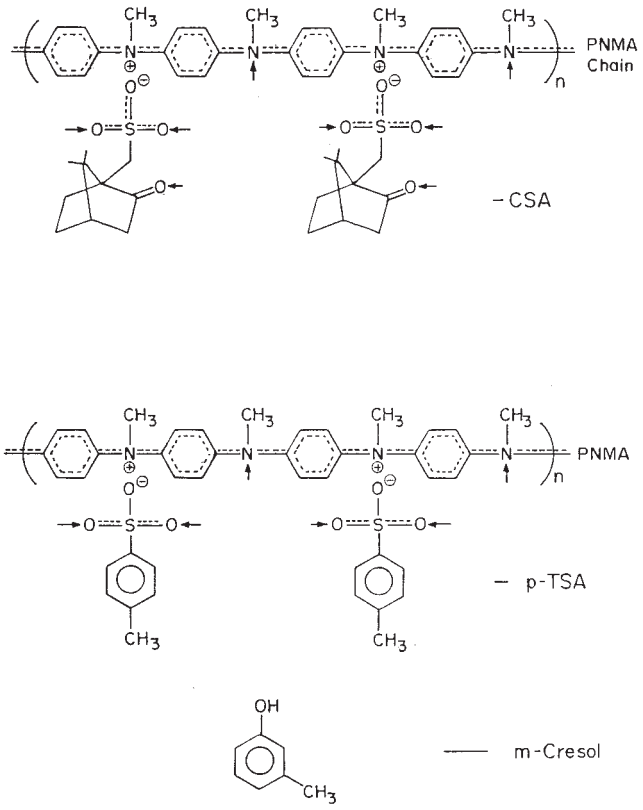

Figure 4 Schematic representation of the possible interaction of the polymer chains with *m*-cresol (the different bonding sites are denoted by arrows).

poly (*N*-methyl aniline) is similar to that of the polyaniline, with characteristic modes of the polyaniline backbone with a very small variation. Also, the presence of well defined peaks at 1731 cm^{-1} and 1031 cm^{-1} related to the C═O and SO_3^- groups shows the efficient incorporation of CSA and *p*-TSA into the polymer backbone.[25] The peak at 2923 cm^{-1}, which appears due to the C-H stretching vibration of the substituent methyl group, is observed exclusively in the poly (*N*-methyl aniline) and is absent in the unsubstituted polyaniline.[26]

We also found that the morphology of the polymer changes depending upon the acid used for the doping. Figures 6 and 7 show micrographs of poly (*N*-methyl aniline) doped with CSA and *p*-TSA, at different magnifications, respectively. The morphology of the polymer synthesized using CSA exhibits exclusively a sponge like structure at 1000 and 2000× [Fig. 6(a,b)]. At higher magnifications, of 4000× [Fig. 6(c)], the clarity of the morphology is found to be further enhanced. It is observed that the sponge like structure is because of aggregation of small uniform sized granules. The appearance of small granules in poly (*N*-methyl aniline) can be explained by considering the steric contribution of the substituent methyl group present on the nitrogen (N) atom. It leads to distortion in the polymer chains, which in turn results in a breakdown of the polymer chain into small granular shaped fragments, appearing as small granules at higher magnification in the micrograph.

The *p*-TSA doped PNMA exhibits a fibrillar type of morphology. At lower magnifications, of 1000 and 2000×, it appears like a bundle of a long fiber; while at higher magnifications, of 4000×, one can clearly see the long fiber having the size of 700 nm throughout the surface of the polymer. From the SEM studies, we can conclude that CSA doped material shows a sponge like morphology, while *p*-TSA doped material offers a long fibrillar morphology to the polymer. Thus, depending upon the type of the dopant, the morphology is found to be varied from sponge like structure to fibrillar in nature.

Figure 8 displays the thermal profile of the poly (*N*-methyl aniline) doped with CSA and *p*-TSA. From the Figure it is observed that the *p*-TSA doped polymer exhibits a three step decomposition pattern similar to that of unsubstituted polyaniline, while the CSA-doped polymer shows a four step decomposition pattern. The first step in the decomposition pattern from RT-100°C is obviously due to the removal of free water molecules/moisture present in the polymer matrix. The second step loss, starting from 120 to 300°C, is mainly because of the loss of the dopant ion from the polymer chains (thermal dedoping). The third step

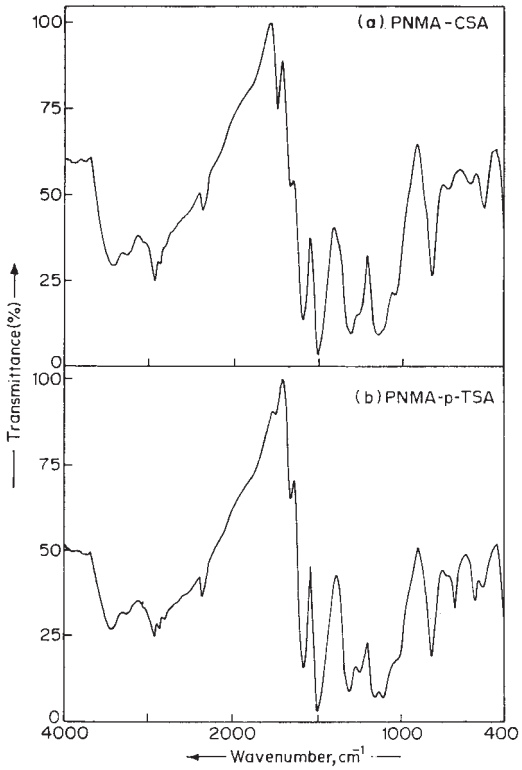

Figure 5 FTIR spectra of poly(*N*-methyl aniline) doped with CSA (a) and *p*-TSA (b).

TABLE I
Characteristic Frequencies of Chemically Synthesized CSA and *p*-TSA Doped Poly(*N*-methyl aniline)

Wavenumber (cm^{-1})		
Poly (*N*-methyl aniline)-CSA	Poly (*N*-methyl aniline)-*p*-TSA	Band characteristics
589.14	562.52	C—H out of plane bending vibration
817.69	815.03	Paradisubstituted aromatic rings indicating polymer formation
1035.22	1035.34	Due to SO_3^- group of the CSA and *p*-TSA
1150.56	1111.23	C—H in plane bending vibration
1309.35	1313.67	Aromatic C—N stretching indicating secondary aromatic amine group
1501.08	1498.72	C—N stretching of benzenoid rings
1588.66	1581.63	C—N stretching of quinoid rings
1733.40	—	>C═O group of CSA
2925.39	2924.97	C—H stretching frequencies characteristic of N—CH_3 groups
3232.12	3233.11	The aromatic C—H stretching
3431.99	3432.01	>N—H stretching vibration

loss, starting from 350°C onwards, is accounted for by the degradation and decomposition of the skeletal polymer backbone after the elimination of the dopant ion.[13] In the CSA doped polymer, the third step weight loss (at 300°C) is attributed to the degradation and decomposition of the smaller chains, while the fourth step (at 400°C) could be due to the breakdown of the longer chains of the polymer. On the other hand, a gradual weight loss with respect to temperature is observed in the *p*-TSA doped PNMA.

In both polymers, rapid weight loss is observed in the third step of the decomposition, over a small temperature range of 350 to 500°C. This is mainly because of the presence of the alkyl substituent present on the nitrogen atom of the polymer backbone. Due to the greater extent of steric effect rendered by this methyl group, loosening of the polymer skeleton requires a less amount of energy to undergo a complete breakdown of the polymer chains. Thus, the incorporation of substituent on the nitrogen atom reduces the thermal stability of the resulting polymer because of the formation of defects in the polymer chains, which favor the degradation and decomposition of the polymer matrix. On comparison of the weight losses in the third step of decomposition, it is observed that 50% of the original weight is stable up to 515°C in CSA doped PNMA; while in *p*-TSA doped PNMA, it is stable up to 570°C. Also, 40% weight is stable up to 900°C in the *p*-TSA doped sample; whereas in the CSA doped sample, it is stable up to only 850°C. Thus, *p*-TSA doped PNMA is thermally more stable than that doped with CSA.

The room temperature solid state conductivities were measured on pressed pellets having a diameter of 1.5 cm using the two probe technique. Table II gives the values. The conductivity of *p*-TSA doped poly(*N*-methyl aniline) is higher than that doped with CSA. The lower conductivity relative to polyaniline may be explained by an increase of the interchain distance and diluting effect of the charge carriers caused by the presence of the bulky methyl group present on the nitrogen atom in the polymer. Consequently, the torsion angle between the repeat units is greater in substituted polyaniline. This explains the noticed decrease in the conductivity. The higher conductivity in *p*-TSA doped PNMA is due to the presence of the fibrillar type of polymer chains, as confirmed by SEM studies, which facilitates close alignment of the polymer chains in a regular fashion. This will increase order in the polymer chains and, hence, easy transportation of the charge carriers across the polymer chains, resulting in the increase of conductivity.

Figure 9 shows the temperature dependent conductivity of poly(*N*-methyl aniline) doped with CSA and *p*-TSA. The conductivity is found to increase with temperature for both samples. The increase in conductivity with increase in temperature is characteristic of "thermal activated behavior." The increase in conductivity would be due to the increase of efficiency of charge transfer between the polymer chains and the dopant with increase in the temperature.[27,28] It can also be suggested that the thermal curing affects the chain alignment of the polymer, which leads to the increase of conjugation length, and that brings about the increase of conductivity. Also, there had to be molecular rearrangement on heating, which made the molecular conformation favorable for electron delocalization.[29,30]

Figure 10 shows the characteristic response of poly(*N*-methyl aniline) doped with CSA and *p*-TSA as a function of relative humidity (% RH). From the Figure, it can be noted that both polymers respond to the % RH by undergoing a change in resistance. The resistance varied almost linearly, from 20% RH to 100% RH, and decreases from low humidity (dry state) to high humidity (wet state).

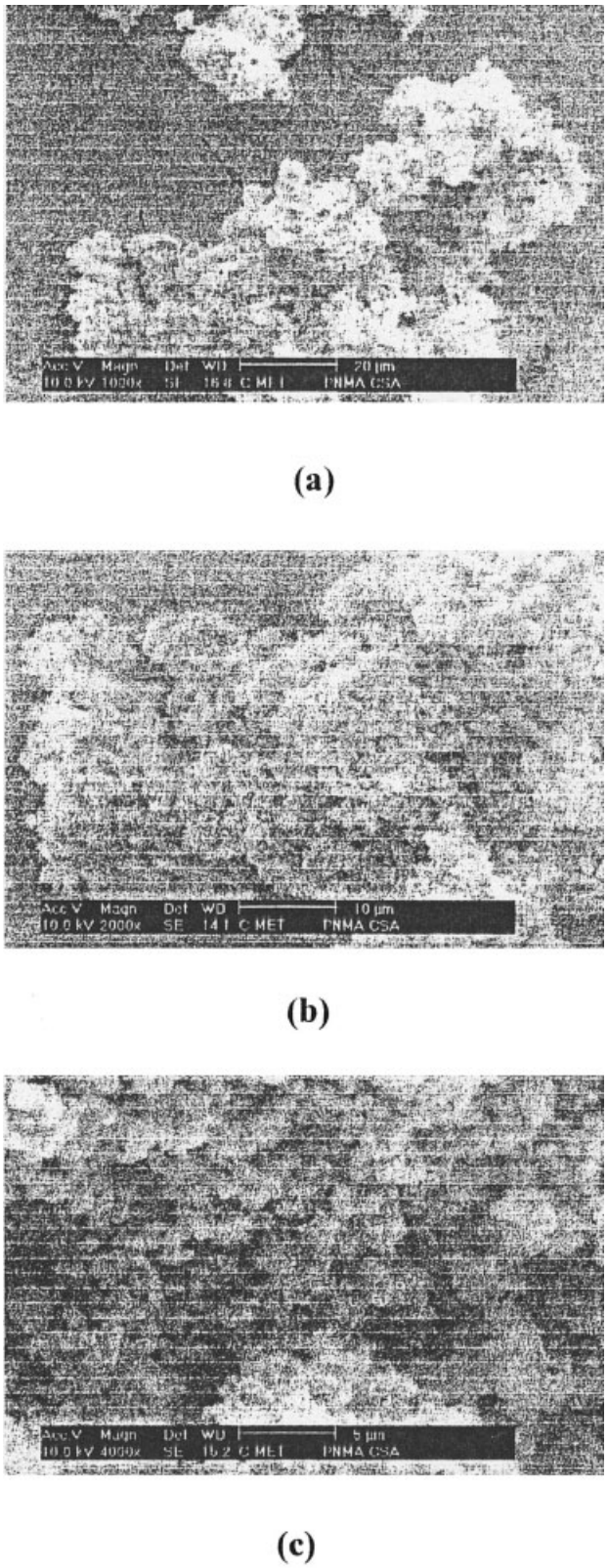

Figure 6 Scanning electron micrographs of poly(*N*-methyl aniline) doped with CSA at (a) 1000×, (b) 2000×, and (c) 4000×.

The decrease in the resistance or increase in the conductivity with increasing humidity can be attributed to the mobility of the dopant ion, which is loosely attached to the polymer chain by weak van der Walls forces of attraction. At low humidity, the mobility of the dopant ion is restricted because under dry condi-

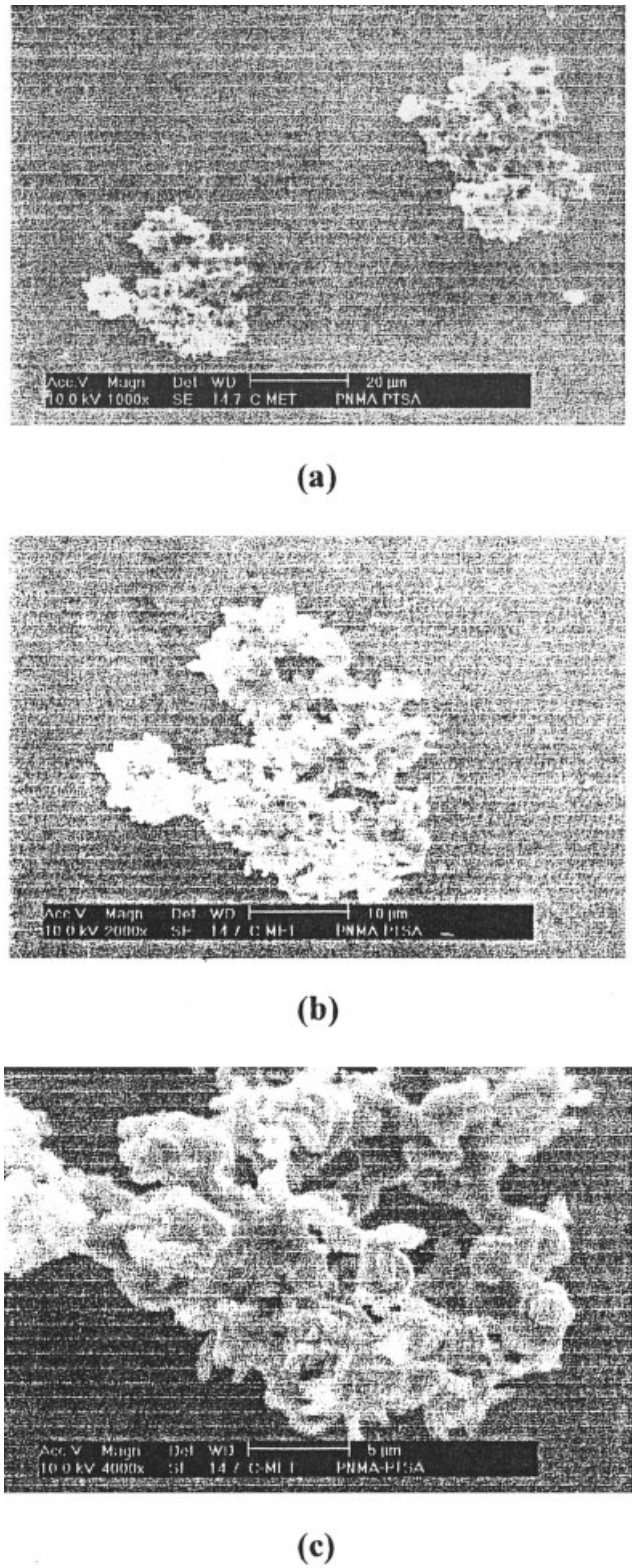

Figure 7 Scanning electron micrographs of poly(*N*-methyl aniline) doped with *p*-TSA at (a) 1000×, (b) 2000×, and (c) 4000×.

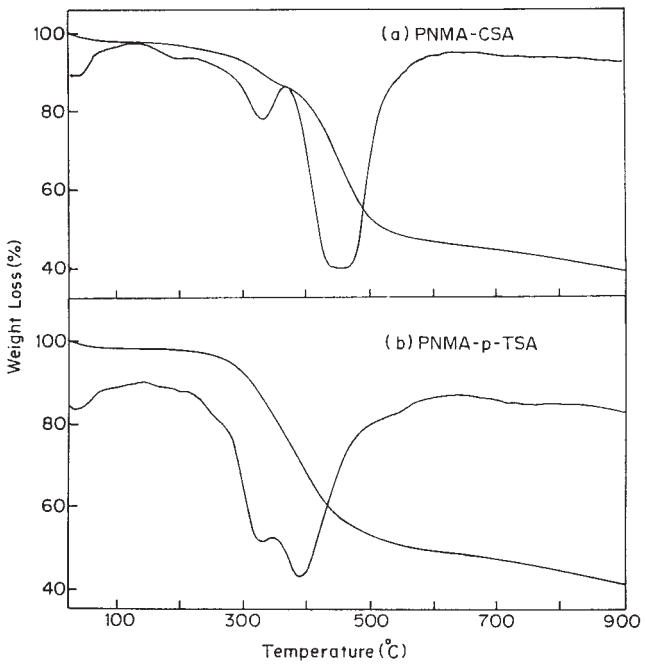

Figure 8 Thermograms of poly(*N*-methyl aniline) doped with (a) CSA and (b) *p*-TSA.

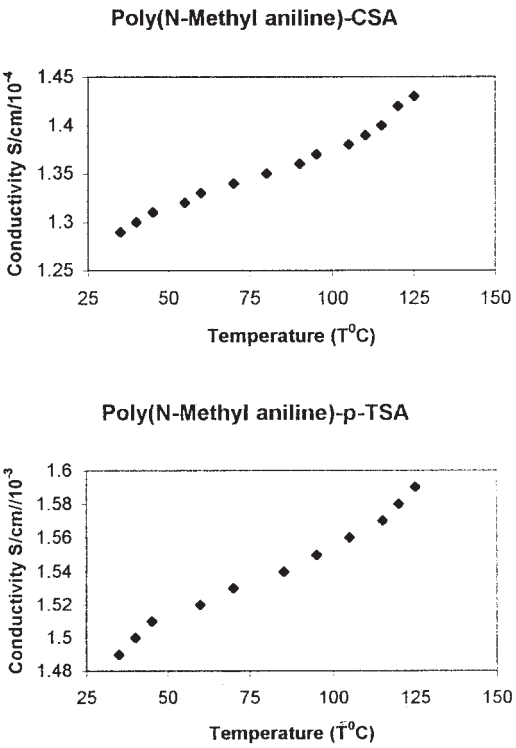

Figure 9 Temperature dependent conductivity plots of poly(*N*-methyl aniline) doped with CSA and *p*-TSA.

tions, the polymer chains would tend to curl up into compact coil form. On the contrary, at high humidity, the polymer absorbs water molecules, and the polymer chains get hydrated. As a result, swelling up of the polymer chains takes place, followed by the uncurling of the compact-coil form into straight chains that are aligned with respect to each other. This geometry of the polymer is favorable for enhanced mobility of the dopant ion or the charge transfer across the polymer chains and, hence, the conductivity.

Furthermore, the water content also plays an important role in the transport properties. Also, it has been reported that the conductivity of a conducting polymer increases when the sample absorbs water molecules/moisture.[31] The water molecules get dissociated into H^+ (OH^-) kind of species and the respective ions behave like reducing agents, which change the effective doping level of the polyaniline. According to Matveeva[32] and Ogura et al.,[33] the interaction of polymers with water is as shown in Scheme 1. According to Scheme 1, water dissociates at the imine center ($HOH \leftrightarrow H^+ + OH^-$) and the proton incorporates into the polymer chain and π-conjugation of aromatic rings, which promotes easier electron transfer. Decrease of resistance with increase in humidity proves the adsorption of water molecules, which makes the polymer more *p*-type in nature, that is, the hole concentration is increased by donation of the lone pair from the conducting complex towards the dopant water molecules. Thus, the partial charge transfer process of conducting species with that of water molecules results in decrease in the sheet resistivity. At higher humidity levels, the mechanism may be different.[34] It has also been proposed that the H_2O molecules may be bound either by two hydrogen bonds—in which case they are fixed—or by a single hydrogen bond—in which case they can rotate. In that case, they are attached either to the polymer or to a fixed H_2O molecule.[31] The two possibilities can be represented as shown in Figure 11.

The almost linear variation with respect to % relative humidity (% RH) can be used in an amplifier circuit for converting the measured values into measurable % RH values. On careful observation of Figure 10, it is clearly seen that poly(*N*-methyl aniline) doped

TABLE II
Room Temperature Conductivity Values of Poly (*N*-Methyl Aniline) Doped with CSA and *p*-TSA

Polymer	Conductivity S/cm
Poly (*N*-methyl aniline)-CSA	1.27×10^{-4}
Poly (*N*-methyl aniline)-*p*-TSA	1.49×10^{-3}

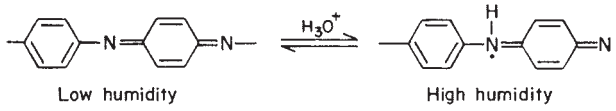

Scheme 1

with CSA shows a linear response from 20% RH to 100% RH. On the other hand, in *p*-TSA doped polymer, the resistance is found to drop from 20% RH up to 60% RH rapidly in a linear fashion. After 60% RH, decrease in the resistance is very small. In other words, we can say that poly(*N*-methyl aniline) doped with *p*-TSA shows a two step sensing response. Thus, poly(*N*-methyl aniline) doped with CSA shows better sensing properties and exhibits good linearity in response, although it is less conducting than that doped with *p*-TSA. Further detailed investigation of response time, hysteresis, and stability is in progress in our laboratory.

CONCLUSIONS

Poly(*N*-Methyl aniline) doped with camphor sulfonic acid (CSA) and *p*-toluene sulfonic acid (*p*-TSA) was synthesized by the *in situ* chemical polymerization method using ammonium persulfate as an oxidizing agent. This is a direct polymerization process for the synthesis of the conducting emeraldine salt phase of the polymer. Formation of mixed phases of polymer, together with the conducting emeraldine salt phase, is confirmed by spectroscopic techniques. SEM studies revealed that PNMA doped with CSA shows a sponge like morphology, while long, uniform size fibers were observed in *p*-TSA doped PNMA. Thermal analysis shows that PNMA doped by *p*-TSA has a three stage decomposition pattern, similar to polyaniline; while CSA-doped PNMA has a four step decomposition pattern. The less conductivity in poly(*N*-methyl aniline) compared to polyaniline is due to the cumulative steric as well as electronic effects of the bulky methyl substituent present on the nitrogen atom. High temperature conductivity measurements show "thermal activated behavior." The almost linear response of poly(*N*-methyl aniline) doped with CSA to the broad range of humidity proves it to be a competent material for a humidity sensor.

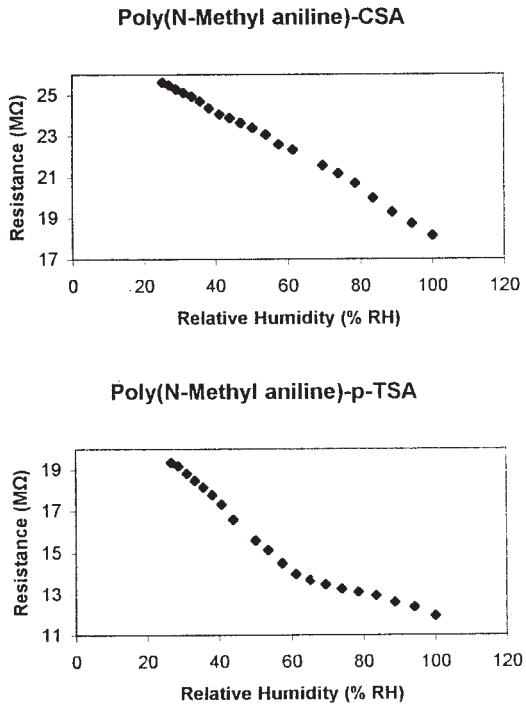

Figure 10 Characteristic response of poly(*N*-methyl aniline) doped with CSA and *p*-TSA for a broad range of humidity (20% RH–100% RH).

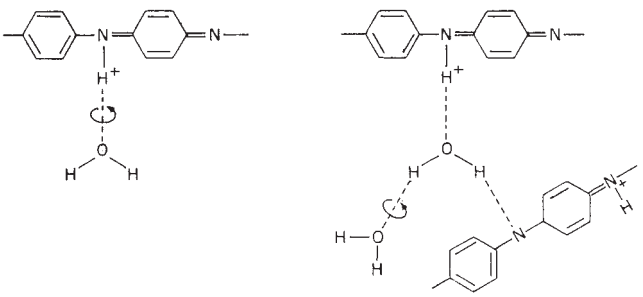

Figure 11 Schematic of the possibilities of hydrogen bonding.

The authors are thankful to Dr. B. K. Das, Executive Director, C-MET, Pune, for his constant encouragement.

References

1. Wang, J.; Wang, D.; Miller, E. K.; Moses, D.; Bazan, G. C.; Heeger, A. J. Macromolecules 2000, 33, 5153.
2. Syed, A. A.; Dinesan, M. K. Talanta 1991, 38, 815.
3. Huang, W. S.; Humphrey, B. D.; MacDiarmid, A. G. J Chem Soc Faraday Trans 1986, 82, 2385.
4. Li, W.; Wan, M. Synth Met 1998, 92, 121.
5. Genies, E. M.; Boyle, A.; Lapkowski, M.; Tsintavis, C. Synth Met 1990, 36, 139.
6. MacDiarmid, A. G.; Chiang, J. C.; Epstein, A. J. Faraday Discuss Chem Soc 1989, 88, 317.
7. Cao, Y.; Smith, P.; Heeger, A. J. Synth Met 1992, 48, 91.
8. Cao, Y.; Smith, P.; Heeger, A. J. Synth Met 1993, 55, 3514.
9. Bracken, E. Sens Review 1997, 17, 291.
10. Maddanimath, T.; Mulla, I. S.; Sainkar, S. R.; Vijaymohanan, K.; Shaikh, K. I.; Patil, A. S.; Vernekar, S. P. Sens Actuators B 2002, 81, 141.
11. Park, S. W.; Kang, J. H.; Park, J. S.; Mun, S. W. Sens Actuators B 2001, 76, 322.
12. Lubentsov, B.; Timofeeva, O.; Saratovskikh, S.; Krinichnyl; Pelekh, A.; Dmitrenka, V.; Khidekel, M. Synth Met 1992, 47, 187.
13. Kulkarni, M. V.; Viswanath, A. K. Eur Polym J 2004, 40, 379.
14. Kulkarni, M. V.; Viswanath, A. K.; Marimuthu, R.; Seth, T. Polym Eng Sci 2004, 44, 1676.
15. Kulkarni, M. V.; Viswanath, A. K.; Marimuthu, R.; Seth, T. J Polym Sci Part A: Polym Chem 2004, 42, 2043.
16. Kulkarni, M. V.; Viswanath, A. K. J Macromol Sci Pure Appl Chem 2004, 41, 1173.
17. Kulkarni, M. V.; Viswanath, A. K.; Mulik, U. P. Mater Chem Phys 2005, 89, 1.
18. (a) Kulkarni, M. V.; Viswanath, A. K.; Marimuthu, R.; Mulik, U. P.; J Mater Sci: Mater Electronics Sensors Actuators B: Chem

2004, 15, 781; (b) Kulkarni, M. V.; Viswanath, A. K. Sensors and Actuators B: Chem 2005, 107, 791.
19. Somani, P. R.; Viswanath, A. K.; Aiyer, R. C.; Radhakrishnan, S. Sens Actuators B 2001, 80, 141.
20. Somani, P. R.; Viswanath, A. K.; Aiyer, R. C.; Radhakrishnan, S. Org Electronics 2001, 2, 83.
21. Moon, D. K.; Padias, A. B.; Hall, H. K. Jr.; Huntoon, T.; Calvert, P. D, Macromolecules 1995, 28, 6205.
22. MacDiarmid, A. G.; Epstein, A. J. Synth Met 1995, 69, 85.
23. Ikkala, O. T.; Pietila, L. O.; Ahjopalo, L.; Osterholm, H.; Passiniemi, P. J. J Chem Phys 1995, 103, 9855.
24. Ikkala, O. T.; Vikki, T.; Passiniemi, P. J.; Osterholm, H.; Osterholm, J. E.; Pietila, L. O.; Ahjopalo, L. Synth Met 1997, 84, 55.
25. Patil, R. C.; Ahmed, M. C.; Ogura, K. Polym J 2002, 32, 466.
26. Manohar, S. K.; MacDiarmid, A. G. Synth Met 1989, 29, E-349.
27. Leclerc, M.; Aparno, G. D.; Zotti, G. Synth Met 1997, 55, 1527.
28. Zuo, F.; Angelopoulos, M.; MacDiarmid, A. G.; Epstein, A. J. Phys Rev B 1987, 36, 3475.
29. Kobayashi, A.; Ishikawa, H.; Amano, K.; Satoh, M.; Hasegawa, E. J Appl Phys 1993, 74, 296.
30. Han, M. G.; Im, S. S. Polymer 2000, 41, 3253.
31. Alix, A.; Lemoine, V.; Nechtschein, M.; Travers, J. P.; Menardo, C. Synth Met 1989, 29, E 457.
32. Matveeva, E. S. Synth Met 1996, 79, 127.
33. Ogura, K.; Saino, T.; Nakayama, M.; Shiigi, H. J Mater Chem 1997, 7, 2363.
34. Jain, S.; Chakane, S.; Samui, A. B.; Krishnamurthy, V. N.; Bhoraskar, S. V. 9th National Seminar on Physics and Technology of Sensors (NSPTS-9), Pune, March 4–6, 2002.